RESEARCH ARTICLE

Potential Biomarkers for Radiation-Induced Renal Toxicity following ^{177}Lu-Octreotate Administration in Mice

Emil Schüler[1]*, Maria Larsson[1], Toshima Z. Parris[2], Martin E. Johansson[3], Khalil Helou[2], Eva Forssell-Aronsson[1,4]

1 Department of Radiation Physics, Institute of Clinical Sciences, Sahlgrenska Cancer Center, Sahlgrenska Academy at the University of Gothenburg, Sahlgrenska University Hospital, Gothenburg, Sweden, **2** Department of Oncology, Institute of Clinical Sciences, Sahlgrenska Cancer Center, Sahlgrenska Academy at the University of Gothenburg, Sahlgrenska University Hospital, Gothenburg, Sweden, **3** Department of Laboratory Medicine, Lund University, SUS Malmö, Malmö, Sweden, **4** Department of Medical Physics and Medical Bioengineering, Sahlgrenska University Hospital, Gothenburg, Sweden

* emil.schuler@gu.se, eschuler@stanford.edu

Abstract

The kidneys are one of the main dose-limiting organs in peptide receptor radionuclide therapy and due to large inter-individual variations in renal toxicity, biomarkers are urgently needed in order to optimize therapy and reduce renal tissue damage. The aim of this study was to investigate the transcriptional, functional, and morphological effects on renal tissue after ^{177}Lu-octreotate administration in normal mice, and to identify biomarkers for radiation induced renal toxicity.

Methods

C57BL/6N mice were i.v. injected with 0, 30, 60, 90, 120, or 150 MBq ^{177}Lu-octreotate (0, 16, 29, 40, 48, and 54 Gy to the kidneys). At 4, 8, and 12 months after administration, radiation-induced effects were evaluated in relation to (a) global transcriptional variations in kidney tissues, (b) morphological changes in the kidneys, (c) changes in white and red blood cell count as well as blood levels of urea, and (d) changes in renal function using ^{99m}Tc-DTPA/^{99m}Tc-DMSA scintigraphy.

Results

In general, the highest number of differentially regulated transcripts was observed at 12 months after administration. The *Cdkn1a*, *C3*, *Dbp*, *Lcn2*, and *Per2* genes displayed a distinct dose-dependent regulation, with increased expression level with increasing absorbed dose. *Ifng*, *Tnf*, and *Il1B* were identified as primary up-stream regulators of the recurrently regulated transcripts. Furthermore, previously proposed biomarkers for kidney injury and radiation damage were also observed. The functional investigation revealed reduced excretion of ^{99m}Tc-DTPA after 150 MBq, an increased uptake of ^{99m}Tc-DMSA at all dose levels compared with the controls, and markedly increased urea level in blood after 150 MBq at 12 months.

Conclusion

Distinct dose-response relationships were found for several of the regulated transcripts. The *Cdkn1a*, *Dbp*, *Lcn2*, and *Per2* genes are proposed as biomarkers for ^{177}Lu-octreotate exposure of kidney. Correlations to functional and morphological effects further confirm applicability of these genes as markers of radiation damage in kidney tissue.

Introduction

The development of biomarkers for clinical practice requires a detailed understanding of the disease under investigation [1]. After exposure to stressors, e.g. radiopharmaceuticals, induced kidney injury is the result of the relationship between, for example, cell dysfunction, cell death, proliferation, inflammation, and recovery. Therefore, these cellular processes need to be better understood in order to identify biomarkers indicative of radiation-induced kidney injury [2].

Therapy with radiolabeled somatostatin (SS) analogues has shown promising results concerning tumor regression, increased overall survival, and improved quality of life for patients with somatostatin receptor (SSTR) overexpressing neuroendocrine tumors [3, 4]. Uptake of radiolabeled SS analogues in normal tissues is generally lower than in tumor tissue [5, 6]. The highest normal tissue uptake takes place in the kidneys which is one of the main critical organs, beside bone marrow, for therapy [7–10]. There is a clear need to define biomarkers of radiation-induced kidney injury in order to avoid adverse effects during this type of therapy.

To assess the applicability of potential biomarkers, their relation to kidney function needs to be established including e.g. glomerular filtration rate (GFR), tubular reabsorption and secretion. Well-established methods to measure GFR include renal inulin clearance and total plasma clearance of ^{51}Cr-EDTA [11]. However, repeated urine and blood sampling is cumbersome on mice after injection of ^{51}Cr-EDTA. Instead scintigraphy might be an alternative to measure renal function [12]. ^{99m}Tc-DTPA is exclusively excreted into the urine by glomerular filtration, without tubular secretion or reabsorption [13]. Tubular reabsorption and secretion is instead preferably measured by ^{99m}Tc-DMSA scintigraphy [14]. The ^{99m}Tc-DMSA uptake process is not entirely known, but seems to include both tubular secretion from blood and glomerular filtration followed by reabsorption [15]. A previous study indicated that ^{99m}Tc-DMSA uptake is mediated by the megalin-cubilin endocytosis which is interesting because it mimics one of the uptake pathways of SS [16].

Upon kidney function disorders, alterations in blood levels of albumin, creatinine, urea, and cystatin C levels may be induced, alterations which might be used as biomarkers of kidney failure [13]. The most commonly used molecular biomarker for the assessment of renal function is serum creatinine. However, the usefulness of serum creatinine in renal injury assessment is probably limited because of a lack of power for the identification of early renal injury and dysfunction, as well as a strong dependence on muscle mass, age, sex, medications, and hydration status [2]. Instead, serum cystatin C has been proposed as marker of GFR and appears to be less dependent of age, sex, and muscle mass, which may indicate a more reliable marker [17]. Other biomarkers for kidney injury have also been proposed, such as KIM-1 and NGAL [18, 19]. However, their role as molecular biomarkers for radiation-induced kidney injury after radiopharmaceutical administration needs to be investigated.

The transcriptional response of normal tissues following radiopharmaceutical administration has previously been investigated following ^{131}I, ^{211}At, and ^{177}Lu exposure [20–24]. It was found that the molecular response is highly dependent on both type of radionuclide used, as

well as time after administration, absorbed dose, and dose rate. Concerning the kidneys, the molecular response 24 h after ^{177}Lu-octreotate administration revealed strong dose-dependent association with metabolic and stress response related processes. Furthermore, recurrent regulation of e.g. *Havcr1* (KIM-1) and *Lcn2* (NGAL) were found, indicating induced kidney injury at these absorbed doses (up to 140 MBq of injected activity). These studies were short-term (3h-7d) and performed on Balb/c mice that are found more radiation sensitive compared with normal mice [24, 25].

In patients treated with ^{177}Lu-octreotate, potential kidney toxicity occurs late after administration [26, 27]. To our knowledge, the molecular mechanisms behind late kidney toxicity have not been studied previously. In order to further our understanding of underlying mechanisms of late kidney toxicity long-term studies on transcriptional regulation after administration should be performed in normal mice, in combination with histological and functional examinations.

The aim of this study was to investigate the transcriptional, morphological and functional effects on renal tissue 4, 8 and 12 months after ^{177}Lu-octreotate administration in normal mice, and to identify potential biomarkers for radiation induced renal toxicity.

Materials and Methods

Radiopharmaceuticals

Preparation of ^{177}Lu-DOTA-Tyr^3-octreotate (^{177}Lu-octreotate) was performed according to the manufacturer's instructions (I.D.B. Holland, Baarle-Nassau, Netherlands). The fraction of peptide bound ^{177}Lu was higher than 99% in the final solution, as determined by instant thin layer chromatography.

^{99m}Tc-DTPA (diethylene-triaminepenta-acetate) and ^{99m}Tc-DMSA (dimercaptosuccinic acid) were acquired from Covidien (Millington, Dublin, Ireland), and preparation was performed according to the manufacturer's instructions.

The activity of the syringes was measured before and after administration with a well-type ionization chamber (CRC-15R; Capintec, IA, USA) to determine the injected activity.

Animal handling

C57BL/6N mice (5–6 weeks old) were acquired from Taconic (Hudson, USA). A total of 45 mice (n = 3 per group) were i.v. injected with 30, 60, 90, 120, and 150 MBq ^{177}Lu-octreotate. Nine mice were injected with saline solution and used as age-matched controls. Mice were killed at 4, 8, or 12 months after injection by cardiac puncture under anesthesia (pentobarbital-natrium, APL, Sweden) followed by blood sample collection and excision of kidneys. One kidney from each animal was subjected to transcriptional microarray analysis, whereas the remaining kidney was used for histological evaluation. Furthermore, 16 mice (n = 4 per group) were i.v. injected with 0, 30, 90, and 150 MBq ^{177}Lu-octreotate and subjected to scintigraphic examination at 4, 8, and 12 months after administration.

This study was carried out in strict accordance with the recommendations on use of laboratory animals and all efforts were made to minimize suffering of the animals. The experimental protocol was approved by the Ethics Committee on Animal Experiments in Gothenburg, Sweden (permit number: 166–204).

Dosimetry

The absorbed dose calculations to the kidneys were based on the Medical Internal Radiation Dose (MIRD) pamphlet 21 formalism [28]:

$$\bar{D}(r_S, T_D) = \frac{\tilde{A}(r_S, T_D)\sum_i E_i Y_i \phi(r_T \leftarrow r_S, E_i, T_D)}{M(r_T, T_D)},$$

where $\tilde{A}(r_S, T_D)$ is the time integrated activity, r_S and r_T the source and target tissue, respectively, T_D is the dose-integration period, E_i is the energy of the ith nuclear transition, Y_i is the number of ith nuclear transitions per nuclear transformation, $\phi(r_T \leftarrow r_S, E_i, T_D)$ is the absorbed fraction, and $M(r_T, T_D)$ is the mass of the target tissue. r_S was set to be the same as r_T in the calculations. $\Sigma_i E_i Y_i$ was approximated to 147 keV, only including electrons emitted. The absorbed fraction, $\phi(r_T \leftarrow r_S, E_i, T_D)$ was set to 0.93 [29]. $\tilde{A}(r_S, T_D)$ was based on biodistribution data on C57BL/6N mice after ¹⁷⁷Lu-octreotate administration [30]. The absorbed dose was calculated to whole kidney.

Transcriptional data processing

Genome-wide transcriptional analysis and data processing has been previously described [24, 31].

Homogenization of the tissue samples was performed with the Mikro-Dismembrator S ball mill (Sartorius Stedim Biotech) and total RNA extraction was performed with the RNeasy Lipid Tissue Mini Kit (Qiagen), according to the instructions of the manufacturer. The quality assessment of the samples was conducted through the NanoDrop ND-1000 and the RNA 6000 Nano LabChip Kit with Agilent 2100 Bioanalyzer (Agilent Technologies), with a RIN cut-off value of 6.

The RNA samples were processed at SCIBLU (Swegene Center for Integrative Biology at Lund University) using MouseRef-8 Whole-Genome Expression Beadchips (Illumina). The image acquisition and analysis were performed with the Illumina BeadArray Reader scanner and BeadScan 3.5.31.17122, respectively.

The web-based BioArray Software Environment (BASE) was used for data preprocessing and quantile normalization. Nexus Expression 3.0 (BioDiscovery, El Segundo, CA, USA) was used for further data analysis using log2-transformed, normalized expression values, and variance filter. Differential expression was determined using the Benjamini-Hochberg method to control the false discovery (FDR-corrected P value < 0.01). A log₂-ratio > 0.58 were considered significant. Generated transcriptional profiles are available from the NCBI's Gene Expression Omnibus (GEO accession number GSE54674).

Further analysis, including up-stream regulators and pathway analysis, was conducted using the IPA software (Ingenuity Systems, Redwood City, USA).

Histological evaluation

The formalin fixed kidneys were processed by standard techniques for embedding in paraffin and sections (2 μm) were stained with haematoxylin-eosin. The evaluation of kidney histology was performed by a kidney pathologist in a blinded fashion.

^{99m}Tc-DTPA and ^{99m}Tc-DMSA scintigraphy

^{99m}Tc-DTPA and ^{99m}Tc-DMSA scintigraphy was performed at 4, 8, and 12 months after ¹⁷⁷Lu-octreotate administration. A single headed gamma camera (ADACT 210, ADAC Laboratories A/S, Aalsborg, Denmark) equipped with medium energy parallel-hole collimator was

used. Images were acquired with a 20% energy-window centered over the 140 keV photon peak, with an image matrix size of 256x256. For calibration, a syringe with known ^{99m}Tc activity was included in each image.

About 55 MBq ^{99m}Tc-DTPA was i.v. injected and posterior 1-minute images were obtained every fifth min between 2.5 and 32.5 min after injection. Two days later, 40 MBq ^{99m}Tc-DMSA was i.v. injected and a posterior 3-minute image was acquired 3h after injection.

Image processing was performed with ImageJ software [32]. Regions-of-interest (ROIs) were outlined for each kidney at 10% of maximal pixel count level, for whole body and around the calibration syringe, and the total number of counts in each ROI was determined. The bladder content was determined at 27.5 min after ^{99m}Tc-DTPA administration. The activity in the kidneys was calculated, assuming similar attenuation for the activity in the kidneys and the calibration syringe.

Statistical analyses with paired Student t-test were used, and $p < 0.05$ was regarded as statistically significant.

Blood analyses

After cardiac puncture, blood was collected in a heparin (Orifarm, Odense, Denmark) coated needle. To assess blood cellular content, whole blood was analyzed by the Sysmex pocH-100i automated hematology system (Sysmex, Kobe, Japan), according to the manufacturer's instructions.

Creatinine and urea levels in whole blood were analyzed using the Reflotron (Roche Diagnostics, Mannheim, Germany) according to the manufacturer's instructions.

Results

Transcriptional response

The absorbed dose to the kidneys was estimated to 16, 29, 40, 48, and 54 Gy after injection of 30, 60, 90, 120, and 150 MBq ^{177}Lu-octreotate.

The number of differentially regulated transcripts ranged from 0 to 188 in kidney cortex, and from 10 to 172 in kidney medulla (Fig 1). A total of 34 and 32 of the differentially regulated transcripts in kidney cortex and medulla, respectively, have previously been suggested associated with kidney injury or radiation damage (Table 1), e.g. *Mmp2*, *Cdkn1a*, and *Ccnd1*. The strongest association with kidney damage-associated markers was found at 8 months for both tissues, with recurrent expression of e.g. *Cdkn1a*, *S100a6*, and *Lcn2*. At 4 and 8 months after injection, the highest number of kidney injury markers and/or radiation markers was found after 150 MBq. At 12 months, the strongest association was observed at 90 and 120 MBq in both tissues.

Several transcripts were frequently regulated at different time points and absorbed doses (Figs 2 and 3). The *Cdkn1a* (cyclin-dependent kinase inhibitor 1A) gene was differentially regulated at all time-points and the majority of activities for both tissues. The *Erg1* gene was also frequently differentially regulated at the higher activities, with the exception of 120 MBq at all time-points. The *Acta2* gene was frequently observed for the higher activities at 8 months, and for the lower activities at 12 months after injection (30–90 MBq). Transcripts with recurrently altered expression levels, which have not previously been associated with kidney injury or radiation injury, included the *Dbp* gene with altered expression in both tissues for 30–90 MBq at 8 and 12 months. In addition, the *C3* (complement component 3) gene was generally differentially regulated for 90–150 MBq at 8 and 12 months. The *Hmgcs2* (3-hydroxy-3-methylglutaryl-Coenzyme A synthase 2) gene was frequently regulated for 30–120 MBq at 12 months in both tissues.
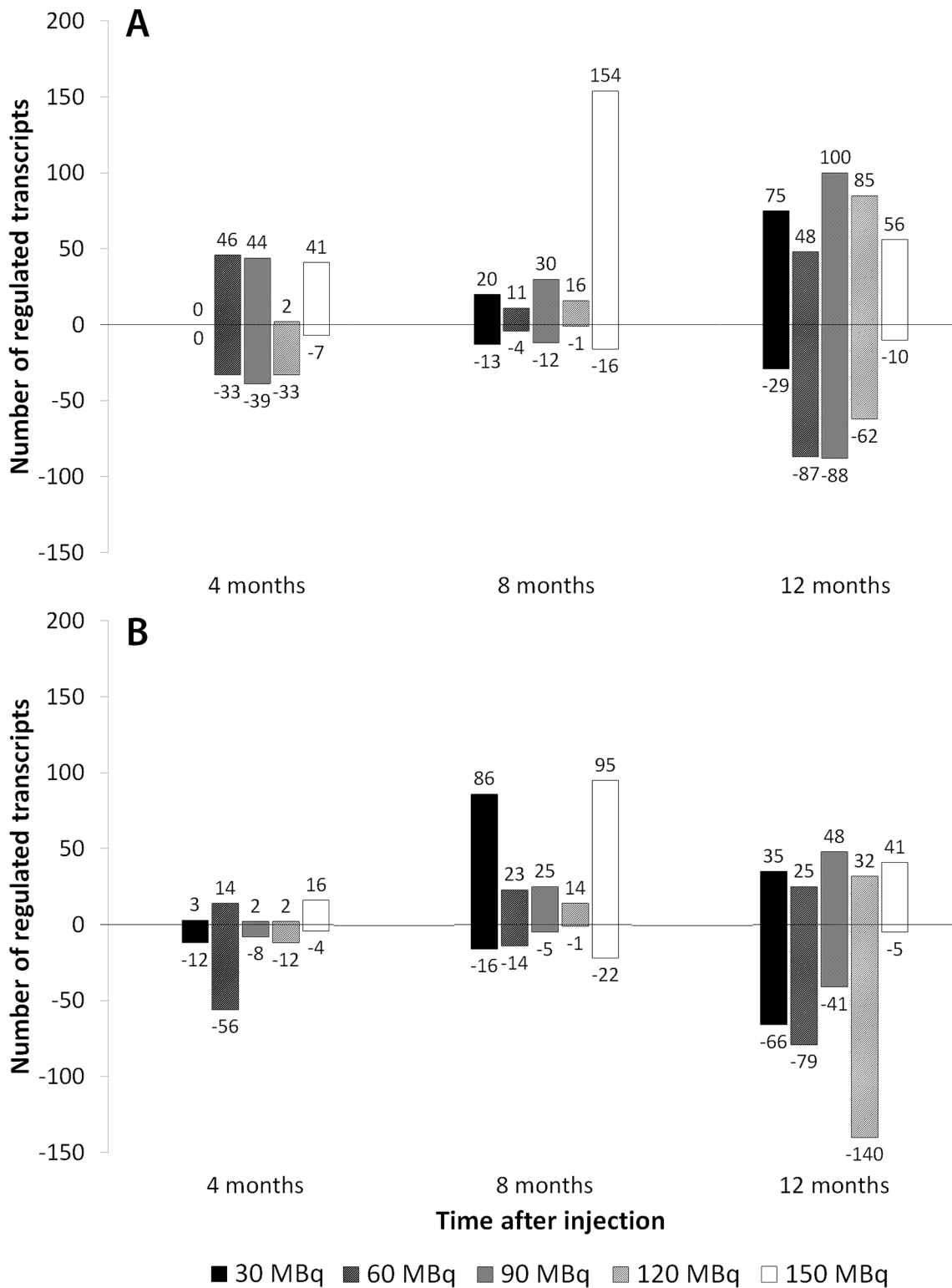
Fig 1. Number of differentially regulated transcripts. Number of differentially regulated transcripts in (a) kidney cortex and (b) kidney medulla 4, 8 and 12 months after administration of 30–150 MBq 177Lu-octreotate. Distribution of up- and down-regulated transcripts is indicated with positive and negative numbers, respectively

doi:10.1371/journal.pone.0136204.g001

Table 1. Radiation responsive genes. Differentially regulated transcripts which have previously been proposed as biomarkers for kidney injury, radiation induced damage, and radiation biodosimetry [33–36]. The log$_2$ratio is shown for each gene.

Time	Kidney Cortex						Kidney Medulla					
	Gene symbol	30 MBq	60 MBq	90 MBq	120 MBq	150 MBq	Gene symbol	30 MBq	60 MBq	90 MBq	120 MBq	150 MBq
4 months	Bcat1*			0.65		0.63	Cyr61*	0.75				
	Egr1*		1.2	1.3		1.2	Egr1*	1.7	1.1	1.1		1.2
	Gdf15*					0.72	Igfbp3*					-0.70
	Hspa1a*					0.80	**Mmp2***					1.0
	Lcn2*					1.0	S100a6*		-0.73			
	Mmp2*					0.83	**Cdkn1a†**		0.69	1.1	1.2	1.8
	Cdkn1a†			1.2	1.49	2.0	**Fos†**	0.91				
	Ccng1‡					0.67	Cxcl12‡		-0.99			
	Gadd45g‡					1.5	Gadd45g‡		-0.69		-0.64	1.2
	Trp53inp1‡					0.70	Tnfrsf21‡		-0.81			
8 months	Akap12*					0.63	Anxa2*					0.62
	Anxa3*					0.88	**Anxa3***					0.78
	Col3a1*					0.65	Col3a1*					0.72
	Col4a1*					0.81	Col4a1*					0.66
	Cxcl1*					1.7	Cxcl1*					1.4
	Cyr61*					0.97	Cyr61*					0.71
	Egr1*					1.7	Egr1*		0.79	1.3		1.8
	Gdf15*				0.97	1.4	Gdf15*					1.2
	Havcr1*					1.6	Havcr1*				1.6	1.3
	Hspa1a*		0.61				Hspa1a*		0.79	1.0		
	Icam1*					0.87	Igfbp3*					-0.77
	Lcn2*				1.8	2.0	Lcn2*		0.86		1.6	1.9
	Lgals3*					0.94	Lgals3*					0.87
	Mmp2*			1.3		1.5	**Mmp2***				1.1	1.0
	S100a6*			1.3		0.83	Mt1*		-0.70			
	Tnfrsf12a*					1.2	S100a6*	-0.72	1.0	1.0		0.97
	Vcam1*					1.6	Tnfrsf12a*					1.1
	Acta2†			0.76		0.82	Vcam1*					1.2
	Cdkn1a†		0.87	1.1	1.5	1.8	Acta2†			0.75		0.76
	Fos†					1.0	**Cdkn1a†**		1.0	1.2	1.5	1.7
	Ccng1‡			0.74		0.93	**Fos†**			0.62		1.2
	Cx3cl1‡					0.70	Cxcl9‡	0.78				0.72
	Cxcl12‡	0.77					**Pcna‡**	0.62				
	Gadd45g‡	0.87					Tnfrsf21‡	-1.0	-1.1			
	Gjb2‡	-0.97		-0.86								
12 months	Acox1*	-0.73	-0.78	-0.72			Acox1*				-0.59	
	Anxa2*			0.77	0.72		Afm*				-0.68	
	Anxa3*			0.64			Col4a1*				0.74	
	Bcat1*			0.75			Lcn2*				0.91	3.2
	Col4a1*			0.68			**Mmp2***			0.66	0.70	
	Cxcl1*					2.7	Acta2†	0.91	0.80	1.1		
	Egr1*				0.65		**Cdkn1a†**	1.3	1.1	1.4	1.1	1.5
	Gdf15*			0.70	0.59		**Ccnd1‡**				0.58	

(Continued)

Table 1. (Continued)

Time	Kidney Cortex						Kidney Medulla				
	Gene symbol	30 MBq	60 MBq	90 MBq	120 MBq	150 MBq	Gene symbol	30 MBq	60 MBq	90 MBq	120 MBq	150 MBq
	Hspa1a*	0.66					Ccng1‡				0.63	
	Lcn2*		0.80	0.76	3.6		Gjb2‡	-0.75				
	Mmp2*			0.84	0.93		Hspe1‡				-0.63	
	Mt1*	-0.64	-0.70				Tnfrsf21‡		-0.93	-0.64		-1.5
	S100a6*	1.3	0.86	1.2	1.0							
	Vcam1*			0.88	0.66	2.1						
	Acta2†	1.1	0.94	1.1								
	Cdkn1a†	1.3	1.0	1.6	1.4	2.0						
	Ccnd1‡			0.65	0.61							
	Gadd45g‡		-0.61									
	Gja1‡	0.81			0.79							
	Gjb2‡	-0.59										
	Lep‡				0.83							
	Tnfrsf21‡		-0.91		-1.0							

* Previously proposed kidney damage marker

† Previously proposed kidney damage marker and ionizing radiation marker

‡ Previously proposed ionizing radiation marker.

Bold indicates that the gene has also been proposed at the protein level to be a potential biodosimeter

doi:10.1371/journal.pone.0136204.t001

The frequently regulated transcripts were identified primarily as potential targets of different cytokines and transcription regulators (Table 2). The up-stream regulators *Ifng* and *Tnf* were most strongly associated with the kidney cortex, whereas *Ifng*, *Il1B*, and *Nr3c1* were most strongly associated with the kidney medulla.

Histological evaluation

The histological evaluation revealed glomerular segmentalization and signs of nodular sclerosis after 150 MBq at 8 months after injection (Fig 4). In addition, at 12 months, prominent nucleol and nuclear fragmentation was observed as well as focal and segmental necrosis for the 150 MBq group. No clear observations of kidney injury were observed at the other activity-levels and time-points investigated.

Scintigraphy

The time-activity curves for ^{99m}Tc-DTPA revealed a statistically significant increased accumulation in the kidneys at 8 and 12 months after ^{177}Lu-octreotate administration for the 90 and 150 MBq groups (Fig 5). At 8 months, a slightly increased and delayed retention of ^{99m}Tc-DTPA was observed after 90 MBq, while after 150 MBq, ^{99m}Tc was accumulated in the kidneys with largely reduced excretion to the urinary bladder (Fig 6). At 12 months, the 90 MBq group showed the same trend of reduction in excretion to the bladder as was shown for 150 MBq at 8 months. Measurements of the 150 MBq group at 12 months were not possible since most of the mice were killed after 8 months due to reduced physical condition. At 4 months, a significantly higher uptake between 2.5 and 12.5 min after ^{99m}Tc administration was observed for the 90 and 150 MBq groups. There was no statistically significant difference in ^{99m}Tc activity in
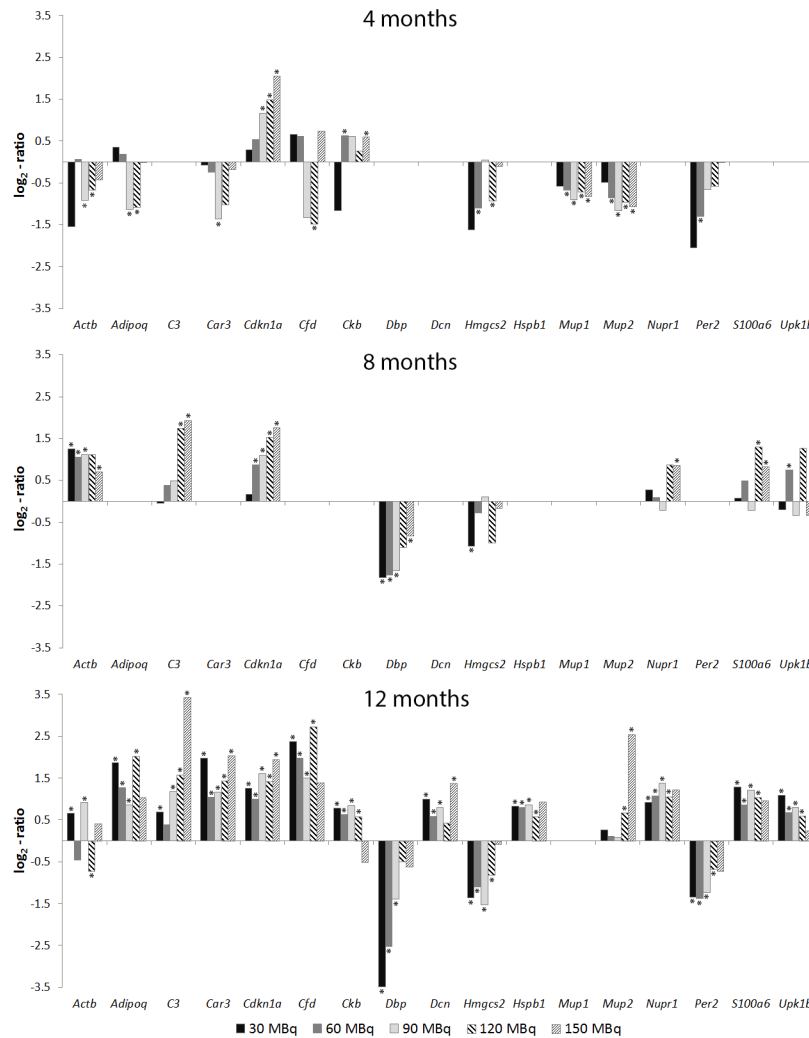
Fig 2. Recurrently regulated transcripts in kidney cortex. Gene expression patterns for differentially regulated transcripts with recurrent expression at one or more time points in kidney cortex 4, 8 or 12 months after administration of 30–150 MBq ^{177}Lu-octreotate. * Statistically significant regulation (see Materials and Methods)

the kidneys between the 30 MBq group and the control group at any time point, except for two time-points at 4 and 12 months (Fig 5).

A statistically significant increase in uptake of ^{99m}Tc-DMSA compared with controls was observed at 4 months for mice injected with 30 and 150 MBq ^{177}Lu-octreotate (p<0.05) (Fig 7). Furthermore, a time-dependent accumulation of the ^{99m}Tc was observed, with increased uptake at 8 and 12 months compared with 4 months.

Blood sample analyses

The mean white blood cell count at 4 months (compared to the control group) was reduced by a factor 2.0, 1.9, and 1.6 after 30, 90, and 150 MBq, respectively (Table 3). No or only minor differences in red blood cell count was detected. Measurements at longer time-points were not possible due to technical difficulties.
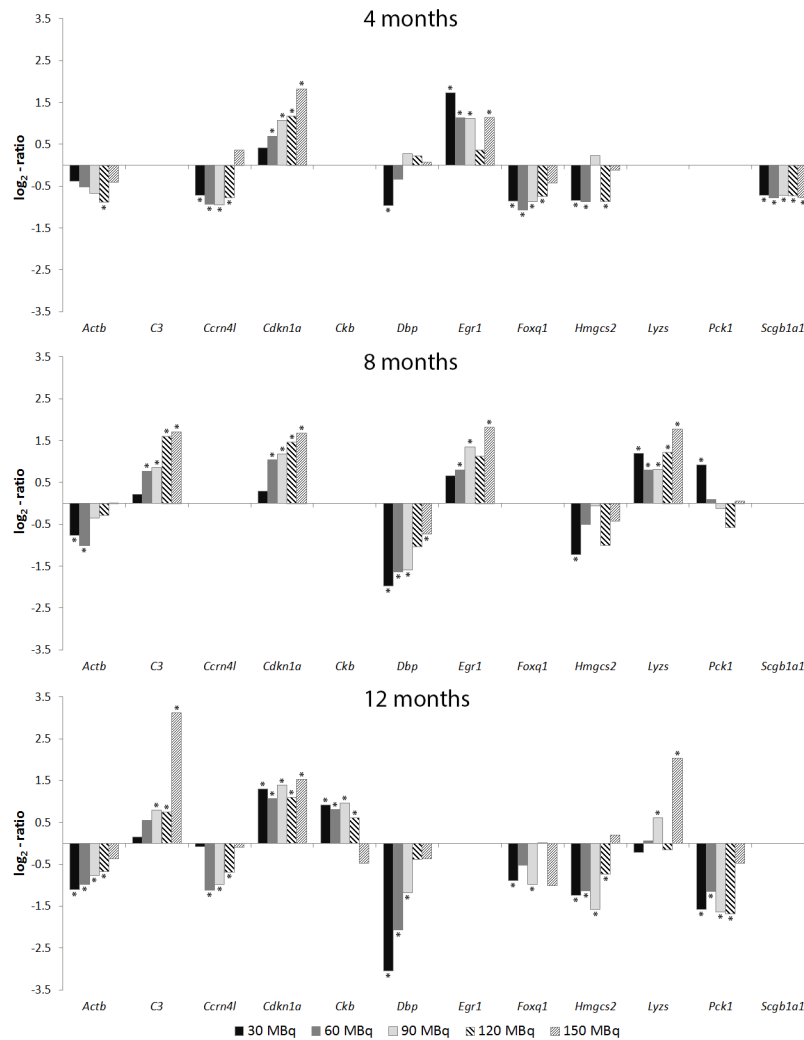
Fig 3. Recurrently regulated transcripts in kidney medulla. Gene expression patterns for differentially regulated transcripts with recurrent expression at one or more time points in kidney medulla 4, 8, or 12 months after administration of 30–150 MBq ^{177}Lu-octreotate. * Statistically significant regulation (see Materials and Methods)

The creatinine levels in blood revealed no or only minor differences compared with controls. A 5-fold increase in blood urea levels were found at 12 months after 150 MBq ($p < 0.05$), whereas lower values were observed at the other time points and activity levels.

Discussion

The present study represents a comprehensive investigation of the long-term transcriptional, functional, and morphological effects of ^{177}Lu-octreotate administration on kidney tissue, one of the main limiting organs in ^{177}Lu-octreotate therapy. Distinct late toxic effects were seen in mice, with reduced kidney function, demonstrated by scintigraphy, morphology, and urea level. Furthermore, the transcriptional analyses revealed a distinct dose-dependent regulation of expression, which correlated with the functional and morphological data.

In the current study, the absorbed dose was calculated to whole kidney. The distribution of the radionuclides in the kidneys is heterogeneous, and previous studies have shown a higher

Table 2. Upstream regulators. Top upstream regulators of transcripts with recurrent expression (cf. Figs 2 and 3) in kidney cortex and medulla

Upstream regulators	Kidney Cortex	Kidney Medulla	Description
Ifng	*Actb, Adipoq, C3, Cdkn1a, Dbp, Hspb1, Nupr1*	*Actb, C3, Cdkn1a, Dbp, Egr1, Pck1*	Interferon gamma, Cytokine
Tnf	*Actb, Adipoq, C3, Cdkn1a, Cfd, Dcn, Per2*	*C3, Cdkn1a, Egr1*	Tumor necrosis factor, Cytokine
Cebpb	*Adipoq, C3, Cdkn1a, Cfd, Dcn, Nupr1*	*C3, Cdkn1a*	CCAAT/enhancer binding protein (C/EBP) beta, Transcription regulator
Il1B	*C3, Cdkn1a, Dbp, Dcn, Hspb1, S100a6*	*C3, Ccrn4l, Cdkn1a, Dbp, Egr1*	Interleukin 1 beta, Cytokine
Cebpa	*Adipoq, C3, Cdkn1a, Cfd, Mup1*		CCAAT/enhancer binding protein (C/EBP) alpha, Transcription regulator
Pparg	*Adipoq, Cdkn1a, Cfd, Hmgcs2*	*Cdkn1a, Hmgcs2, Pck1*	Peroxisome proliferator-activated receptor gamma, Ligand-dependent nuclear receptor
Erbb2	*Actb, Cdkn1a, Hspb1, S100a6*		Erythroblastic leukemia viral oncogene homolog 2, Kinase
Hoxa10	*Actb, Adipoq, Cdkn1a, Cfd*	*Actb, Cdkn1a*	Homeobox A10, Transcription regulator
Ins1	*Actb, Adipoq, Cdkn1a, Cfd*		Insulin I, Hormone
Lep	*Adipoq, Cdkn1a, Cfd, Per2*	*Cdkn1a, Pck1*	Leptin, Growth factor
Psen1	*Actb, C3, Ckb, Dbp, Nupr1*		Presenilin 1, Peptidase
NFkB (complex)	*C3, Cdkn1a, Dbp, Hspb1*	*C3, Cdkn1a, Dbp, Egr1*	NFkB (complex)
Hras	*Actb, Cdkn1a, Hspb1*	*Actb, Cdkn1a, Egr1, Pck1*	Harvey rat sarcoma viral oncogene homolog, Enzyme
Edn1	*Actb, Adipoq, Nupr1*	*Egr1*	Endothelin 1, Cytokine
Egfr	*Actb, Cdkn1a, Hspb1*	*Actb, Cdkn1a, Egr1*	Epidermal growth factor receptor, Kinase
Nr3c1		*Actb, Cdkn1a, Hmgcs2, Pck1*	Nuclear receptor subfamily 3 C1, Ligand-dependent nuclear receptor

doi:10.1371/journal.pone.0136204.t002

uptake in the kidney cortex compared to medulla at early time points after injection (24h) [8, 37], with concentrations of at least 50–60% in the outer medulla compared to cortex. However, gender dependencies have also been found, where female mice showed higher uptake in the outer medulla compared with the cortex [37]. Due to these discrepancies, and possible mouse strain dependencies, no more detailed tissue dosimetry in the kidneys was performed. Furthermore, the number of animals in the present study was limited to 3–4 per group. While a higher number of animals per group would result in a stronger power to the analysis, the similar genotype of this inbred mouse strain (C57BL/6N) together with tightly controlled working conditions have previously shown a strong reproducibility of the results with 3 animals per group. Unpublished data from our group has also shown that the similarity between the animals in gene expression at the current cut offs used was between 60 and 86%. Due to these facts and ethical considerations, three animals per group were chosen for the transcriptional response analysis.

Several of the differentially regulated transcripts identified in the present study have previously been proposed as biomarkers of radiation damage and kidney injury [19, 33–35, 38–40]. In the present study *Cdkn1a* gene was differentially regulated in 12 of the 15 analyzed groups in kidney cortex, and 13 of the 15 analyzed groups in kidney medulla. The *Cdkn1a* gene is a cycline dependent kinase inhibitor highly involved in cell cycle progression and has previously been shown to be consistently regulated in response to ionizing radiation [33–35]. The *Cdkn1a* gene has also been found to be up-regulated shortly after acute renal failure [38]. In the present study, a dose-response relationship was found for both kidney cortex and medulla at all the time-points studied, with increased transcriptional levels with increased absorbed dose. The transcriptional levels for the *C3* (complement component 3) and *Dbp* (albumin promoter
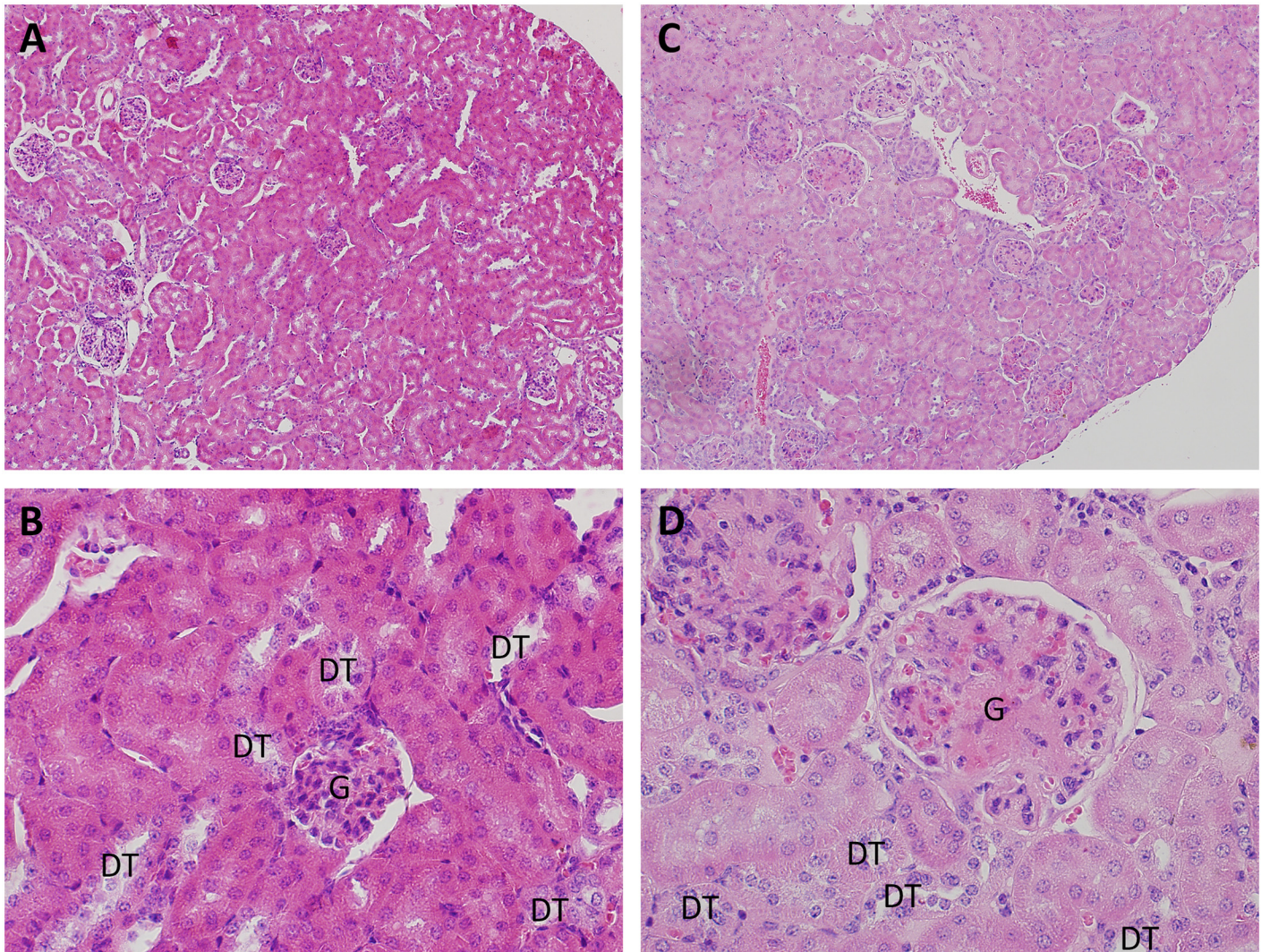
Fig 4. Kidney histology. Kidney histology in control animals as well as in animals where no histological changes were seen at (a) 10x magnification and (b) 40x magnification. The glomeruli are normocellular, with open capillary loops. No signs of segmentalization, necrosis or sclerosis were seen. The tubular, interstitial, and vascular compartments were all without histological changes, no signs of necrosis or inflammation were noted. The histological changes associated with the group receiving 150 MBq at 12 months are shown at (c) 10x magnification and (d) 40x magnification. The changes were localized to the glomeruli. These displayed focal signs of segmental sclerosis and segmentalization of the glomeruli, indicating cellular injury to the mesangium and glomerular capillaries. Edemtatous closure of the capillary loops was noted. Furthermore, the nuclei displayed degenerative changes with polymorphism and nuclear fragmentation, potentially indicating detrimental radiation effects. In a fraction of the glomeruli, signs of segmental fibrinoid necrosis were seen, again underscoring acute injury to the glomeruli. Tubules, interstitium and vasculature showed no signs of injury in these tissues. Staining by standard hematoxylin and eosin. The glomeruli are depicted with"G" and the distal tubules with"DT".

doi:10.1371/journal.pone.0136204.g004

binding protein) genes also exhibited an absorbed dose dependence for both tissues, whereas the *Per2* (periodic circadian clock 2) and *Actb* (actin, beta) genes showed a dose-response relationship in kidney cortex and medulla, respectively. These genes have not previously been associated with radiation damage or kidney induced injury, which may indicate the specificity of these genes in the response to administration of specific radiopharmaceuticals.

The pathway analysis of the recurrently regulated transcripts predicted the *Ifng* and *Tnf* genes in kidney cortex, and the *Ifng*, *Il1B*, and *Nr3c1* genes in kidney medulla as the most highly associated up-stream regulators. The *Ifng*, *Tnfa*, and *Il1* genes have been shown to be involved in "danger" signaling following irradiation, with guidance of orchestration of tissue
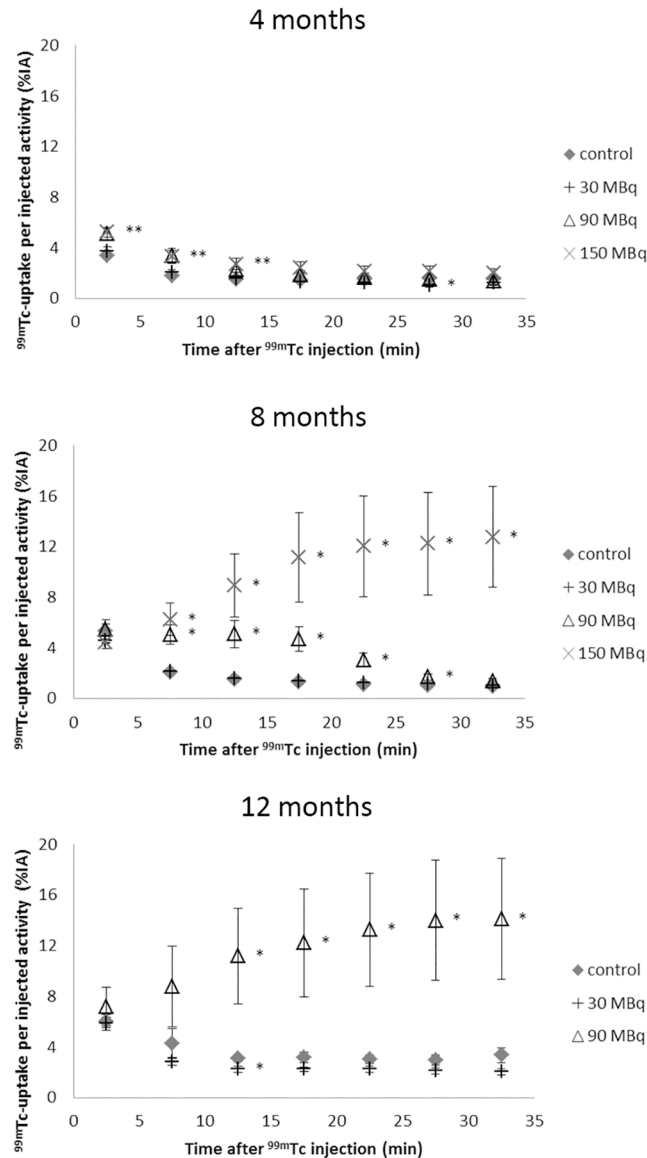
Fig 5. ^{99m}Tc-DTPA scintigraphy. Results from ^{99m}Tc-DTPA scintigraphy performed 4, 8, and 12 months after administration of 0, 30, 90 or 150 MBq ¹⁷⁷Lu-octreotate. The kidney uptake is presented as percent of injected activity. Error bars represent SEM and * indicates statistically significant difference compared with controls ($p < 0.05$), and at 4 months the ** indicates statistical significance for the 90 and 150 MBq groups.

repair [41]. These genes are also involved in cell cycle arrest, cell survival, DNA repair, and senescence [41]. The *Nfkb* complex was also identified as an up-stream regulator, which have been found to be one of the most frequently activated transcription factors by radiation exposure [41–43]. Taken together, these data indicate the importance of transcription factors and cytokine regulation in the response to kidney exposure to ¹⁷⁷Lu-octreotate.

An ideal biomarker for radiation-induced kidney injury should preferably be organ specific and originate from the damaged cells. The dose-response relationship of the biomarker should be directly dependent on the extent of damage, and the change in transcriptional expression should be expressed early after insult [44]. These criteria are of the highest concern to optimize individualized patient treatment. Several of the genes in the present study have also been
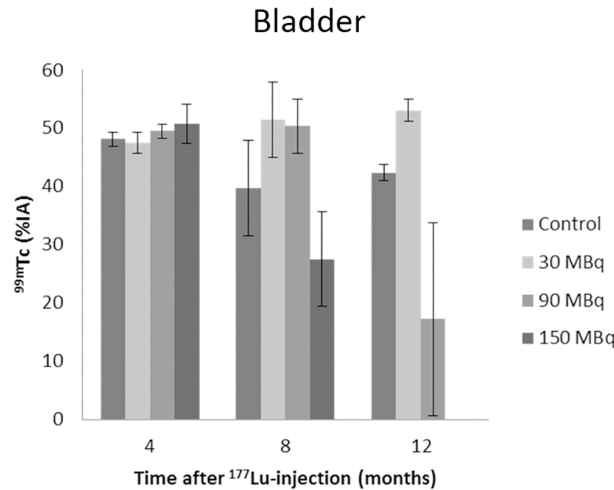
Bladder

Fig 6. Urinary bladder content following ^{99m}Tc-DTPA administration. Urinary bladder content at 27.5 min after ^{99m}Tc-DTPA administration. Scintigraphy was performed at 4, 8, and 12 months after administration of 30–150 MBq ^{177}Lu-octreotate. Kidney uptake is presented as percent of injected activity. Error bars represent SEM

doi:10.1371/journal.pone.0136204.g006

previously found to be differentially expressed at earlier time points than the 4–12 months studied here. The *Car3*, *Cdkn1a*, *Dbp*, *Hmgcs2*, *Mup2*, *Per2*, *S100a6*, and *Upk1b* genes and the *Actb*, *Adipoq*, *Car3*, *Cdkn1a*, *Cfd*, *Ckb*, *Dbp*, *Hmgcs2*, *Nupr1*, *Per2*, and *Upk1b* genes were differentially regulated at 24h after ^{177}Lu-octreotate administration in the kidney cortex and medulla, respectively [31]. The *Cdkn1a* gene showed increased expression with increased absorbed dose also at this early time point in both kidney cortex and medulla. The *Dbp* and *Hmgcs2* genes were differentially regulated at all dose levels studied (0.13–13 Gy) in both tissues, and the *Per2* gene was differentially regulated at absorbed doses between 0.34 and 13 Gy. Already at this early time point (24h after administration), the consistent change in transcriptional levels for several of these genes indicated their potential utility as biomarkers of internal exposure to radionuclides and renal tissue injury.
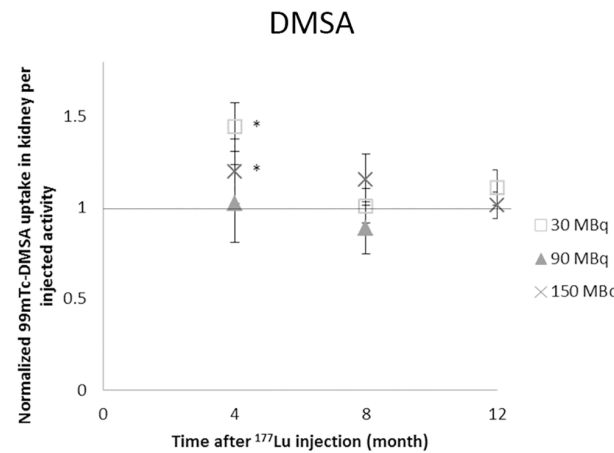
DMSA

Fig 7. ^{99m}Tc-DMSA scintigraphy. Results from ^{99m}Tc-DMSA scintigraphy performed 4, 8, and 12 months after ^{177}Lu-octreotate administration. The kidney uptake is presented as percent of injected activity normalized to controls. Error bars represent SEM and * indicates statistically significant difference compared with controls (p<0.05).

doi:10.1371/journal.pone.0136204.g007

Table 3. Overview of the results. Overview of the results concerning body weight, blood cell count, urea and creatinine blood levels, 99mTc-DTPA and 99mTc-DMSA scintigraphy, and histology. The results are presented as test divided by control (given as percent)

Days after therapy	IA	Body weight (time of death)	White blood cell count	Red blood cell count	Urea	Creatinine	99mTc-DTPA*	99mTc-DMSA	Histology
4 months	30 MBq	110%	50%	99%	130%	100%	66% (27.5 min)	140%	Normal
	60 MBq	98%	ND	ND	97%	100%	ND	ND	Normal
	90 MBq	110%	53%	94%	91%	100%	87% (32.5 min)	100%	Normal
	120 MBq	99%	ND	ND	92%	100%	ND	ND	Normal
	150 MBq	89%	63%	95%	91%	100%	59% (32.5 min)	120%	Normal
8 months	30 MBq	90%	ND	ND	230%	100%	62% (32.5 min)	100%	Normal
	60 MBq	110%	ND	ND	140%	100%	ND	ND	Normal
	90 MBq	100%	ND	ND	140%	100%	270% (12.5 min)	89%	Normal
	120 MBq	100%	ND	ND	280%	100%	ND	ND	Normal
	150 MBq	85%	ND	ND	280%	100%	450% (27.5 min)	110%	Abnormal
12 months	30 MBq	98%	ND	ND	110%	100%	160% (17.5 min)	110%	Normal
	60 MBq	120%	ND	ND	82%	100%	ND	ND	Normal
	90 MBq	110%	ND	ND	140%	100%	910% (27.5 min)	ND	Normal
	120 MBq	110%	ND	ND	160%	100%	ND	ND	Normal
	150 MBq	110%	ND	ND	520%	110%	ND	100%	Abnormal

*Values in parenthesis indicates time after 99mTc-DTPA injection where highest deviation from control was observed

ND = not done

doi:10.1371/journal.pone.0136204.t003

The histological evaluation revealed clear signs of kidney toxicity at the highest activity level investigated (150 MBq, 54 Gy) at 8 and 12 month after administration. The effects in the present study concerned the glomeruli with sclerosing and segmentalization (injury of glomerular capillaries and mesangium) of the glomerular tuft. In addition, at 12 months, signs of cell death could also be observed in the glomeruli in the form of nuclear fragmentation and segmental necrosis. In addition, signs of inflammation were seen. No changes regarding tubules, interstitium or other vessels were observed. These results are in contrast to previously published morphological effects of 177Lu-octreotate on rats (46–92 Gy, 109 days after injection) and nude mice (35–58 Gy, 6 months after injection) [45, 46], demonstrating mainly tubulointerstitial changes after 177Lu-octreotate administration. These consisted of inhomogeneous nuclei formation, apoptosis, and necrotic cells in the proximal and distal tubules as well as flattening of tubular epithelium, loss of brush border, dilation, and empty lumina in a dose-dependent manner after 177Lu-octreotate administration, respectively. In contrast, no or only very mild changes of the glomeruli was observed in these studies.

99mTc-DTPA scintigraphy clearly revealed changes in kidney function with increased amount of 177Lu-octreotate administered and with time after administration. At 4 months after injection no difference in filtration or excretion rate could be observed in any of the groups. At 8 months, an altered time-activity curve was observed for the 90 MBq group, while for the 150 MBq group an accumulation of 99mTc in the kidneys was observed with no or altered emptying into the bladder. At 12 months, few of the animals in the 150 MBq group were alive. The reduced excretion of 99mTc for the 90 MBq group at 12 months was similar to that observed for the 150 MBq group at 8 months, indicating a longer time until renal function loss at reduced activity. No effects on renal clearance curves were observed for the 30 MBq group at any time-point.

In general, the time-activity curve of the kidneys after 99mTc-DTPA administration shows a rapid uptake phase for 1–3 minutes followed by a slow excretion phase when 99mTc is transported to the bladder [14]. The slope of the uptake phase is correlated with GFR. However, due to practical issues, the initial uptake-phase could not be measured in the present study, and the scintigraphic data represent the excretion of 99mTc-DTPA. In a previous study on rats using 111In-DTPA to measure renal function 100–120 days after administration of 460 MBq 177Lu-octreotate, a reduced maximal uptake of 111In in the kidneys compared with untreated controls was found [15]. In the present study we did not measure the maximal uptake due to technical issues, but found a reduced excretion from the kidneys in the most exposed groups. To our knowledge, a rise in the excretion phase of the renal time-activity-curve of 99mTc-DTPA has not been previously observed after 177Lu-octreotate administration. However, one reason behind such results from 99mTc-DTPA scintigraphy is nephrolithiasis [47]. Calculi in kidneys or ureters may develop from metabolic imbalance in electrolytes. In the present study, a strong association with sodium, calcium, and potassium ion binding was observed among the differentially regulated genes. This observation was most prominent at later time points (8–12 months) at the higher absorbed doses delivered (40–54 Gy), which could imply an electrolyte imbalance in the kidney tissues.

99mTc-DMSA scintigraphy revealed no reduction in uptake for any of the groups. Instead a significant increase in 99mTc-uptake was observed at 4 months after 30 and 150 MBq. The kidney uptake of 99mTc-DMSA after 177Lu-octreotate administration has previously been studied in rats [15, 45]. A clear dose-dependent decrease in 99mTc-DMSA uptake was then observed 109–146 days after administration of 278 and 555 MBq 177Lu-octreotate (9.9, and 1.4%IA, respectively, vs. 23%IA in control), indicating tubular damage after the highest injected activity [45]. Furthermore, increased 99mTc accumulation was found in the outer medulla with increased injected activity [45]. In the present study, no statistically significant reduction in uptake was observed at any time-point or 177Lu activity level investigated, despite the functional obstruction observed with 99mTc-DTPA. However, renal or ureter calculi might reduce the 99mTc-DMSA excretion from the kidneys and hide an otherwise reduced kidney uptake [48].

No functional effects were found in the 16 Gy group, but were clearly evident in the 40 Gy group. Thus, the tolerance dose in mice after a single administration of 177Lu-octreotate would be found in the range 16–40 Gy, which is within the range previously reported for both mice and humans [26, 46]. It should be noted that the kidneys would most probably tolerate a higher exposure after fractionated therapy. Furthermore, it is interesting to note that no altered levels of creatinine were detected and clear histological manifestations were only seen at the highest absorbed dose (54 Gy) at 8 and 12 months after administration. This would indicate a possible higher tolerance dose for the kidneys in these mice, compared to the radiosensitive Balb/c mice previously used for toxicity assessments [46]. Furthermore, a distinct dose response relationship was observed for several of the regulated transcripts of, e.g. the *Cdkn1a*, *Dbp*, and *Per2* genes. Together with the functional morphological data, these transcriptional variations were correlated to functional impairment and injury. In a previous study, these transcriptional variations

were observed already at 24h after injection of ^{177}Lu-octreotate [31]. Thus, altered regulation of these genes may serve as biomarkers that might potentially predict injury already at early time points and the ability to follow the progression of the induced injury. However, further studies are needed to establish this correlation. In addition, the protein expression levels of these genes in kidney tissues, blood, and urine also need to be studied to establish their clinical utility.

Conclusions

In the present study, a comprehensive investigation of the transcriptional, functional, and morphological effects of administration of high amounts of ^{177}Lu-octreotate on normal kidney tissue was performed. A strong and diverse transcriptional response was observed, and the functional investigations revealed clear negative effects on renal function, with enhanced effects with absorbed dose and time after administration. Furthermore, the gene expression studies revealed several potentially useful biomarkers, e.g. *Cdkn1a*, *C3*, *Dbp*, *Lcn2*, and *Per2*, that might be used as early predictors of late renal injury. Further studies are needed to evaluate their clinical usefulness.

Author Contributions

Conceived and designed the experiments: ES ML EFA. Performed the experiments: ES ML. Analyzed the data: ES ML TZP MEJ. Contributed reagents/materials/analysis tools: MEJ KH EFA. Wrote the paper: ES ML TZP MEJ KH EFA.

References

1. Hewitt SM, Dear J, Star RA. Discovery of protein biomarkers for renal diseases. J Am Soc Nephrol. 2004; 15(7):1677–89. PMID: 15213255

2. Adiyanti SS, Loho T. Acute Kidney Injury (AKI) biomarker. Acta Med Indones. 2012; 44(3):246–55. PMID: 22983082

3. Khan S, Krenning EP, van Essen M, Kam BL, Teunissen JJ, Kwekkeboom DJ. Quality of life in 265 patients with gastroenteropancreatic or bronchial neuroendocrine tumors treated with [177Lu-DOTA0, Tyr3]octreotate. Journal of nuclear medicine. 2011; 52(9):1361–8. doi: 10.2967/jnumed.111.087932 PMID: 21795361

4. Sward C, Bernhardt P, Ahlman H, Wangberg B, Forssell-Aronsson E, Larsson M, et al. [177Lu-DOTA 0-Tyr 3]-octreotate treatment in patients with disseminated gastroenteropancreatic neuroendocrine tumors: the value of measuring absorbed dose to the kidney. World J Surg. 2010; 34(6):1368–72. doi: 10.1007/s00268-009-0387-6 PMID: 20066413

5. Forssell-Aronsson E, Bernhardt P, Nilsson O, Tisell LE, Wangberg B, Ahlman H. Biodistribution data from 100 patients i.v. injected with 111In-DTPA-D-Phe1-octreotide. Acta oncologica. 2004; 43(5):436–42. PMID: 15360047

6. Forssell-Aronsson EB, Nilsson O, Bejegard SA, Kolby L, Bernhardt P, Molne J, et al. 111In-DTPA-D-Phe1-octreotide binding and somatostatin receptor subtypes in thyroid tumors. Journal of nuclear medicine. 2000; 41(4):636–42. PMID: 10768564

7. Forssell-Aronsson E, Spetz J, Ahlman H. Radionuclide Therapy via SSTR: Future Aspects from Experimental Animal Studies. Neuroendocrinology. 2013; 97(1):86–98. doi: 10.1159/000336086 PMID: 22572526

8. Melis M, Krenning EP, Bernard BF, Barone R, Visser TJ, de Jong M. Localisation and mechanism of renal retention of radiolabelled somatostatin analogues. Eur J Nucl Med Mol Imaging. 2005; 32 (10):1136–43. PMID: 15912401

9. Barone R, Borson-Chazot F, Valkema R, Walrand S, Chauvin F, Gogou L, et al. Patient-specific dosimetry in predicting renal toxicity with (90)Y-DOTATOC: relevance of kidney volume and dose rate in finding a dose-effect relationship. Journal of nuclear medicine. 2005; 46 Suppl 1:99S–106S. PMID: 15653658

10. Vegt E, de Jong M, Wetzels JF, Masereeuw R, Melis M, Oyen WJ, et al. Renal toxicity of radiolabeled peptides and antibody fragments: mechanisms, impact on radionuclide therapy, and strategies for prevention. Journal of nuclear medicine. 2010; 51(7):1049–58. doi: 10.2967/jnumed.110.075101 PMID: 20554737

11. Medeiros FS, Sapienza MT, Prado ES, Agena F, Shimizu MH, Lemos FB, et al. Validation of plasma clearance of 51Cr-EDTA in adult renal transplant recipients: comparison with inulin renal clearance. Transpl Int. 2009; 22(3):323–31. doi: 10.1111/j.1432-2277.2008.00799.x PMID: 19055616

12. Assadi M, Eftekhari M, Hozhabrosadati M, Saghari M, Ebrahimi A, Nabipour I, et al. Comparison of methods for determination of glomerular filtration rate: low and high-dose Tc-99m-DTPA renography, predicted creatinine clearance method, and plasma sample method. Int Urol Nephrol. 2008; 40 (4):1059–65. doi: 10.1007/s11255-008-9446-4 PMID: 18690545

13. Thomas C, Thomas L. Renal failure—measuring the glomerular filtration rate. Dtsch Arztebl Int. 2009; 106(51–52):849–54. doi: 10.3238/arztebl.2009.0849 PMID: 20062583

14. Daniel GB, Mitchell SK, Mawby D, Sackman JE, Schmidt D. Renal nuclear medicine: a review. Vet Radiol Ultrasound. 1999; 40(6):572–87. PMID: 10608684

15. Melis M, de Swart J, de Visser M, Berndsen SC, Koelewijn S, Valkema R, et al. Dynamic and static small-animal SPECT in rats for monitoring renal function after 177Lu-labeled Tyr3-octreotate radionuclide therapy. Journal of nuclear medicine. 2010; 51(12):1962–8. doi: 10.2967/jnumed.110.080143 PMID: 21078795

16. Weyer K, Nielsen R, Petersen SV, Christensen EI, Rehling M, Birn H. Renal uptake of 99mTc-dimercaptosuccinic acid is dependent on normal proximal tubule receptor-mediated endocytosis. Journal of nuclear medicine: official publication, Society of Nuclear Medicine. 2013; 54(1):159–65.

17. Narvaez-Sanchez R, Gonzalez L, Salamanca A, Silva M, Rios D, Arevalo S, et al. Cystatin C could be a replacement to serum creatinine for diagnosing and monitoring kidney function in children. Clin Biochem. 2008; 41(7–8):498–503. doi: 10.1016/j.clinbiochem.2008.01.022 PMID: 18280806

18. Han WK, Bailly V, Abichandani R, Thadhani R, Bonventre JV. Kidney Injury Molecule-1 (KIM-1): a novel biomarker for human renal proximal tubule injury. Kidney Int. 2002; 62(1):237–44. PMID: 12081583

19. Hoffmann D, Adler M, Vaidya VS, Rached E, Mulrane L, Gallagher WM, et al. Performance of novel kidney biomarkers in preclinical toxicity studies. Toxicol Sci. 2010; 116(1):8–22. doi: 10.1093/toxsci/kfq029 PMID: 20118187

20. Rudqvist N, Parris TZ, Schuler E, Helou K, Forssell-Aronsson E. Transcriptional response of BALB/c mouse thyroids following in vivo astatine-211 exposure reveals distinct gene expression profiles. EJNMMI research. 2012; 2(1):1–12. doi: 10.1186/2191-219X-2-1 PMID: 22251281

21. Rudqvist N, Schuler E, Parris TZ, Langen B, Helou K, Forssell-Aronsson E. Dose-specific transcriptional responses in thyroid tissue in mice after (131)I administration. Nuclear medicine and biology. 2015; 42(3):263–8. doi: 10.1016/j.nucmedbio.2014.11.006 PMID: 25496975

22. Langen B, Rudqvist N, Parris TZ, Schuler E, Spetz J, Helou K, et al. Transcriptional response in normal mouse tissues after i.v. (211)At administration—response related to absorbed dose, dose rate, and time. EJNMMI research. 2015; 5:1. doi: 10.1186/s13550-014-0078-7 PMID: 25853007

23. Langen B, Rudqvist N, Parris TZ, Schuler E, Helou K, Forssell-Aronsson E. Comparative analysis of transcriptional gene regulation indicates similar physiologic response in mouse tissues at low absorbed doses from intravenously administered 211At. Journal of nuclear medicine: official publication, Society of Nuclear Medicine. 2013; 54(6):990–8.

24. Schuler E, Rudqvist N, Parris TZ, Langen B, Spetz J, Helou K, et al. Time- and dose rate-related effects of internal Lu exposure on gene expression in mouse kidney tissue. Nuclear medicine and biology. 2014; 41(10):825–32. doi: 10.1016/j.nucmedbio.2014.07.010 PMID: 25156037

25. Schuler E, Rudqvist N, Parris TZ, Langen B, Helou K, Forssell-Aronsson E. Transcriptional response of kidney tissue after 177Lu-octreotate administration in mice. Nuclear medicine and biology. 2014; 41 (3):238–47. doi: 10.1016/j.nucmedbio.2013.12.001 PMID: 24434014

26. Bodei L, Cremonesi M, Ferrari M, Pacifici M, Grana CM, Bartolomei M, et al. Long-term evaluation of renal toxicity after peptide receptor radionuclide therapy with 90Y-DOTATOC and 177Lu-DOTATATE: the role of associated risk factors. Eur J Nucl Med Mol Imaging. 2008; 35(10):1847–56. doi: 10.1007/s00259-008-0778-1 PMID: 18427807

27. Bodei L, Kidd M, Paganelli G, Grana CM, Drozdov I, Cremonesi M, et al. Long-term tolerability of PRRT in 807 patients with neuroendocrine tumours: the value and limitations of clinical factors. Eur J Nucl Med Mol Imaging. 2014.

28. Bolch WE, Eckerman KF, Sgouros G, Thomas SR. MIRD pamphlet No. 21: a generalized schema for radiopharmaceutical dosimetry—standardization of nomenclature. Journal of nuclear medicine: official publication, Society of Nuclear Medicine. 2009; 50(3):477–84.

29. Miller WH, Hartmann-Siantar C, Fisher D, Descalle MA, Daly T, Lehmann J, et al. Evaluation of beta-absorbed fractions in a mouse model for 90Y, 188Re, 166Ho, 149Pm, 64Cu, and 177Lu radionuclides. Cancer biotherapy & radiopharmaceuticals. 2005; 20(4):436–49.

30. Schuler E, Osterlund A, Forssell-Aronsson E. The amount of injected Lu-octreotate strongly influences biodistribution and dosimetry in C57BL/6N mice. Acta oncologica. 2015:1–9.

31. Schuler E, Rudqvist N, Parris TZ, Langen B, Helou K, Forssell-Aronsson E. Transcriptional response of kidney tissue after (177)Lu-octreotate administration in mice. Nuclear medicine and biology. 2014; 41 (3):238–47. doi: 10.1016/j.nucmedbio.2013.12.001 PMID: 24434014

32. Schneider CA, Rasband WS, Eliceiri KW. NIH Image to ImageJ: 25 years of image analysis. Nat Methods. 2012; 9(7):671–5. PMID: 22930834

33. Snyder AR, Morgan WF. Gene expression profiling after irradiation: clues to understanding acute and persistent responses? Cancer Metastasis Rev. 2004; 23(3–4):259–68. PMID: 15197327

34. Chaudhry MA. Biomarkers for human radiation exposure. Journal of biomedical science. 2008; 15 (5):557–63. doi: 10.1007/s11373-008-9253-z PMID: 18454354

35. Filiano AN, Fathallah-Shaykh HM, Fiveash J, Gage J, Cantor A, Kharbanda S, et al. Gene expression analysis in radiotherapy patients and C57BL/6 mice as a measure of exposure to ionizing radiation. Radiation research. 2011; 176(1):49–61. doi: 10.1667/RR2419.1 PMID: 21361780

36. Marchetti F, Coleman MA, Jones IM, Wyrobek AJ. Candidate protein biodosimeters of human exposure to ionizing radiation. Int J Radiat Biol. 2006; 82(9):605–39. PMID: 17050475

37. Melis M, Krenning EP, Bernard BF, de Visser M, Rolleman E, de Jong M. Renal uptake and retention of radiolabeled somatostatin, bombesin, neurotensin, minigastrin and CCK analogues: species and gender differences. Nuclear medicine and biology. 2007; 34(6):633–41. PMID: 17707803

38. Perco P, Pleban C, Kainz A, Lukas A, Mayer G, Mayer B, et al. Protein biomarkers associated with acute renal failure and chronic kidney disease. Eur J Clin Invest. 2006; 36(11):753–63. PMID: 17032342

39. Vaidya VS, Ferguson MA, Bonventre JV. Biomarkers of acute kidney injury. Annu Rev Pharmacol Toxicol. 2008; 48:463–93. PMID: 17937594

40. Nickolas TL, Barasch J, Devarajan P. Biomarkers in acute and chronic kidney disease. Curr Opin Nephrol Hypertens. 2008; 17(2):127–32. doi: 10.1097/MNH.0b013e3282f4e525 PMID: 18277143

41. McBride WH, Chiang CS, Olson JL, Wang CC, Hong JH, Pajonk F, et al. A sense of danger from radiation. Radiat Res. 2004; 162(1):1–19. PMID: 15222781

42. Pajonk F, McBride WH. Ionizing radiation affects 26s proteasome function and associated molecular responses, even at low doses. Radiother Oncol. 2001; 59(2):203–12. PMID: 11325450

43. Li Q, Verma IM. NF-kappaB regulation in the immune system. Nat Rev Immunol. 2002; 2(10):725–34. PMID: 12360211

44. Cruz DN, Goh CY, Haase-Fielitz A, Ronco C, Haase M. Early biomarkers of renal injury. Congest Heart Fail. 2010; 16 Suppl 1:S25–31. doi: 10.1111/j.1751-7133.2010.00163.x PMID: 20653708

45. Forrer F, Rolleman E, Bijster M, Melis M, Bernard B, Krenning EP, et al. From outside to inside? Dose-dependent renal tubular damage after high-dose peptide receptor radionuclide therapy in rats measured with in vivo (99m)Tc-DMSA-SPECT and molecular imaging. Cancer biotherapy & radiopharmaceuticals. 2007; 22(1):40–9.

46. Svensson J, Molne J, Forssell-Aronsson E, Konijnenberg M, Bernhardt P. Nephrotoxicity profiles and threshold dose values for [(177)Lu]-DOTATATE in nude mice. Nuclear medicine and biology. 2012; 39 (6):756–62. doi: 10.1016/j.nucmedbio.2012.02.003 PMID: 22445743

47. Hecht S, Lawson SM, Lane IF, Sharp DE, Daniel GB. (99m)Tc-DTPA diuretic renal scintigraphy in dogs with nephroureterolithiasis. Can Vet J. 2010; 51(12):1360–6. PMID: 21358928

48. Ritchie G, Wilkinson AG, Prescott RJ. Comparison of differential renal function using technetium-99m mercaptoacetyltriglycine (MAG3) and technetium-99m dimercaptosuccinic acid (DMSA) renography in a paediatric population. Pediatr Radiol. 2008; 38(8):857–62. doi: 10.1007/s00247-008-0908-8 PMID: 18551288